JACS
JOURNAL OF THE AMERICAN CHEMICAL SOCIETY
Article
pubs.acs.org/JACS

Microfluidic Studies of CO_2 Sequestration by Frustrated Lewis Pairs

Dan Voicu,[†,#] Milad Abolhasani,[‡,#] Rachelle Choueiri,[†] Gabriella Lestari,[†] Caroline Seiler,[†] Gabriel Menard,[†] Jesse Greener,[§] Axel Guenther,[‡] Douglas W. Stephan,[†] and Eugenia Kumacheva[†,⊥,∥,*]

[†]Department of Chemistry, University of Toronto, 80 Saint George Street, Toronto, Ontario M5S 3H6, Canada

[‡]Department of Mechanical and Industrial Engineering, University of Toronto, 5 King's College Road, Toronto, Ontario M5S 3G8, Canada

[§]Département de Chimie, Université Laval, Pavillon Alexandre-Vachon local 1220, av. De la Médecine, Québec QC G1V 0A6, Canada

[⊥]Institute of Biomaterials and Biomedical Engineering, University of Toronto, 164 College Street, Toronto, Ontario M5S 3G9, Canada

[∥]Department of Chemical Engineering and Applied Chemistry, University of Toronto, 200 College Street, Toronto, Ontario M5S 3E5, Canada

Supporting Information

ABSTRACT: Frustrated Lewis pairs (FLPs) comprising sterically hindered Lewis acids and bases offer the capability to reversibly capture CO_2 under mild reaction conditions. The determination of equilibrium constants and thermodynamic properties of these reactions should enable assessment of the efficiency of a particular FLP system for CO_2 sequestration and provide insights for design of new, efficient formulations of FLP catalysts for CO_2 capture. We have developed a microfluidic approach to studies of FLP–CO_2 reactions, which provides their thermodynamic characterization that is not accessible otherwise. The approach enables the determination of the equilibrium reaction constants at different temperatures, the enthalpy, the entropy, and the Gibbs energy of these reactions, as well as the enhancement factor. The microfluidic methodology has been validated by applying it to the well-characterized reaction of CO_2 with a secondary amine. The microfluidic approach can be applied for fundamental thermodynamic studies of other gas–liquid reactions.

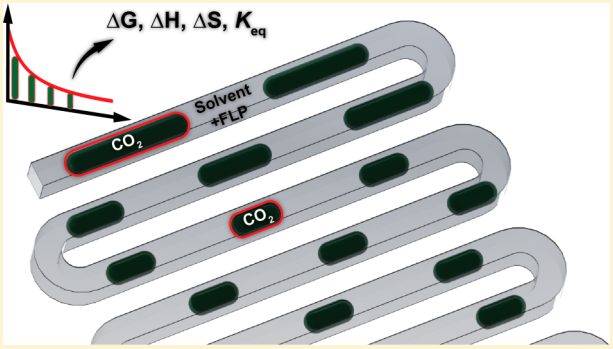

INTRODUCTION

Elevated levels of carbon dioxide (CO_2) in the atmosphere are clearly influencing the progression of global warming. Strategies to manage atmospheric CO_2 concentrations include reducing emissions, sequestration and storage (e.g., in underground aquifers), or utilization of CO_2 as a C_1 chemical feedstock.[1−3] The conversion of CO_2 to products such as formic acid and carbon monoxide[4] or to readily usable fuels such as methanol[5,6] remains a challenge due to the relatively low reactivity and high thermal stability of the CO_2 molecule. While a series of transition metal systems have been reported to effect reduction chemistry of CO_2,[7−11] a unique alternative involves the use of frustrated Lewis pairs (FLPs).[12−14] These systems, comprising sterically hindered Lewis acids and bases, act in concert to capture CO_2 under mild reaction conditions.[15] Moreover, tuning the Lewis acidity and basicity of the FLPs alters their reactivity in reactions with CO_2 from reversible sequestration to stoichiometric and even catalytic reduction to methanol[16] or CO.[17−20]

Strategies to predict and design FLPs capable of the effective sequestration and activation of CO_2 necessitate a deeper understanding of the factors that influence the reaction. To this end, the deliberate studies of the effects of FLP structure, concentrations, and reaction temperatures on the reactivity of FLP reagents are required. As the initial FLPs afforded reversible binding to CO_2, the determination of equilibrium constants and thermodynamic parameters of these reactions should enable assessment of the efficiency of a particular FLP system for CO_2 sequestration and provide predictive insights for design strategies targeting new and efficient formulations of FLP catalysts for CO_2 capture and reduction. Currently used batch-scale characterization methods[21,22] for gas–liquid reactions involving CO_2 are time-consuming and plagued with an insufficient control over gas–liquid interfaces and diffusion control challenges associated with the large volumes of the reactors used. Measurements of a particular physical or chemical property require a relatively large quantity of reagents. Common spectroscopic characterizations of reaction products may be challenged by chemical exchange processes with the atmosphere. Moreover, when equilibrium constants of FLP–CO_2 reactions are high, the equilibrium thermodynamic

Received: November 20, 2013
Published: February 20, 2014

   dx.doi.org/10.1021/ja411601a | J. Am. Chem. Soc. 2014, 136, 3875−3880

characterization cannot be achieved using batch-scale methods.[23]

Recently, the utilization of microfluidic (MF)-based platforms has been proposed to address some of these challenges by dramatically shrinking the dimensions of the reaction vessel from *centimeters* to *micrometers*, thereby reducing the diffusion length and time scales. Integration of in-line characterization tools with different MF devices has enabled high-throughput screening of the physical and chemical processes.[24−30] In particular, a reduced mass transfer limitation and well-defined interfacial areas achieved in gas−liquid segmented flows have been utilized for chemical[31] and physical[32−35] screening of gas−liquid processes involving CO_2.

In the present paper, we report a MF strategy for fundamental thermodynamic studies of the reaction of CO_2 with FLP reagents. Using a MF approach, we calculated equilibrium constants of this reaction at different temperatures, assessed the thermal stability of the adduct, and determined the thermodynamic characteristics of the reaction, such as the enthalpy, entropy, and the Gibbs free energy. The proposed MF method can be used to acquire thermodynamic data for FLP−CO_2 reactions in 10−15 min and can be applied to fundamental studies of other reactions that include reactive gases.

EXPERIMENTAL SECTION

The reagents tri-*tert*-butylphosphine, tBu$_3$P, and chlorobis(pentafluorophenyl)borane, ClB$(C_6F_5)_2$, were synthesized as described elsewhere[23] and dissolved in bromobenzene to various concentrations. Bromobenzene was purchased from Caledon (Canada) and distilled. The solutions of FLP reagents were prepared on the day of the MF experiments and stored in a glovebox (1.2−2 ppm O_2). The solutions of individual FLP reagents in bromobenzene were supplied to the MF reactor from two 1 mL gastight syringes (SGE Analytical Science), using the same syringe pump.

The configuration and dimensions of the MF reactor are shown in Figure S1, Supporting Information. Prior to MF experiments, the MF reactor was purged with dry CO_2 for 10 min at 2 psig to remove air. An inverted microscope (Olympus IX71) coupled to a CCD camera (Photometrics CoolSnap ES) was used for optical characterization of the CO_2 bubbles (plugs) and liquid segments (slugs). ImagePro (Media Sybernetics) software was used to acquire multiple sequences of bright-field images of the segmented flow on-chip. Analysis of the image sequence was carried out using a custom-developed MATLAB-based image processing code, which automatically measured the CO_2 plug length and plug position in a region of interest.[34,35]

Physical dissolution of CO_2 in bromobenzene and in solutions of FLP reagents in bromobenzene was examined using attenuated total reflection Fourier transform infrared (ATR-FTIR) spectroscopy (Vertex 70, Bruker Corp.). Opus 6.5 software was used for spectral analysis.

The glass MF reactor was dried prior to each set of experiments to remove traces of water. Carbon dioxide gas was supplied from a gas tank at the pressure of 118.5 kPa using a digital servo pressure controller. The pressure drop along the microchannel was calculated based on the CO_2 plug velocity, void fraction, microchannel length, liquid viscosity, and the atmospheric pressure of 101.3 kPa at the outlet of the reactor (see Supporting Information, S2). The individual solutions of ClB$(C_6F_5)_2$ and tBu$_3$P in bromobenzene with equal molar concentration were supplied to the MF reactor at a flow rate of 2.5 μL/min (the total volumetric flow rate of the mixed reagent solution was 5 μL/min). The total FLP concentration, C_{FLP}, in the mixed solution was changed from 0 to 50 mM. Experiments were performed at temperatures, T, of 273, 283, 293, 303, and 313 K.

RESULTS AND DISCUSSION

Figure 1a shows the chemical reaction of CO_2 with the FLP reagents, that is, ClB$(C_6F_5)_2$ and tBu$_3$P, leading to the FLP−

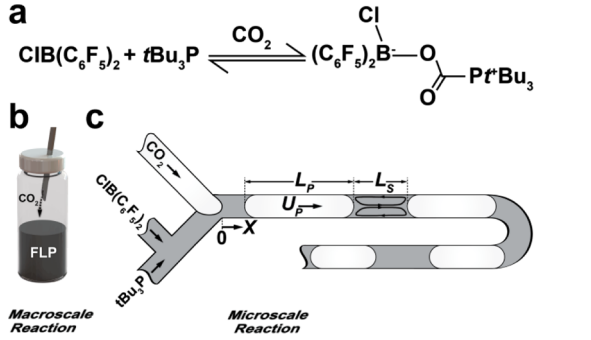

Figure 1. Reversible FLP−CO_2 reaction conducted in a MF reactor. (a) Reaction of FLP reagents, ClB$(C_6F_5)_2$ and tBu$_3$P, with CO_2 in bromobenzene forming the FLP−CO_2 adduct. (b) Schematic of the batch-scale experiment. (c) Illustration of the CO_2 plugs and liquid slugs of FLP reagents with lengths L_P and L_S, respectively, forming at the Y-junction.

CO_2 adduct. Figure 1b illustrates the reaction conducted in a macroscopic format. The process involves bubbling CO_2 into the FLP solution at a fixed pressure, which is followed by the isolation, drying, and analysis of the precipitated product, ClB$(C_6F_5)_2$−CO_2−tBu$_3$P. Generally, one experiment takes ∼2 h from reaction to analysis. The isolated product may undergo a facile loss of CO_2, which is accelerated with increasing temperature. Figure 1c illustrates the same reaction conducted in the continuous mode in a MF reactor using alternating flow of CO_2 plugs and liquid reagent segments (slugs). In our work, the solution of FLP reagents in bromobenzene and the CO_2 gas were supplied via two inlets into the MF reactor. The ClB$(C_6F_5)_2$ and tBu$_3$P reagents were mixed in-line, using a T-junction, before entering the MF device. The liquid reagents and CO_2 converged at the Y-junction, where the gas stream periodically broke up to produce gaseous CO_2 plugs separated by liquid reagent slugs. Following dissolution of CO_2 in an adjacent liquid slug, it reacted with the FLP reagents. As a result of these two processes, the gaseous CO_2 plugs shrank. Two recirculation zones inside each liquid segment enhanced mixing and mass transfer of CO_2 molecules into the liquid phase by convective transport (Figure 1c).

The total change in dimensions of the CO_2 plugs was determined by three factors: (i) the drop in pressure along the microchannel, (ii) the physical dissolution of CO_2 in bromobenzene, and (iii) the chemical reaction of CO_2 with FLP reagents (Supporting Information, Figure S2). The first effect led to the expansion of CO_2 plugs, while the other two effects led to gaseous plug shrinkage. At equilibrium, the physical dissolution and reaction-induced reduction in CO_2 plug dimensions were temporarily balanced by the pressure drop along the channel, and the size of the CO_2 plugs remained constant.

In the course of experiments, we monitored the variation in the length of CO_2 plugs, L_P, when CO_2 dissolved in the adjacent liquid segment with the length L_S (L_S remained approximately constant). By accounting for the expansion of the gas plug due to the pressure drop,[32] we evaluated the amount of CO_2 transferred from the gas plugs to the liquid slugs. Since the initial size of the generated CO_2 plugs was

dx.doi.org/10.1021/ja411601a | J. Am. Chem. Soc. 2014, 136, 3875−3880

sufficiently large to retain their plug-like shape after CO_2 dissolution, we assumed that the gas plugs and the liquid slugs moved with the same velocity, and in this manner, we converted the distance traveled by the plugs and slugs into reaction time, t (see Supporting Information, S2).

Assuming an ideal gas behavior, we calculated the time-dependent volume of CO_2 plugs, V_P, and the number of moles of CO_2, $nCO_2(t)$, in the plug at time t as

$$nCO_2(t) = \frac{PV_P}{RT} \quad (1)$$

where P is the pressure in the plug after accounting for pressure drop at each location, R is the gas constant (R = 8.314 J mol^{-1} K^{-1}), and T is the temperature of the system. The total number of moles of CO_2 transferred from the plug equaled the number of CO_2 moles entering the liquid segment, and the concentration of CO_2 in the liquid was calculated as

$$C_{tot}(t) = \frac{nCO_2(t=0) - nCO_2(t)}{V_S} \quad (2)$$

where $C_{tot}(t)$ is the total concentration of CO_2 in the liquid slug at time t; $nCO_2(t = 0)$ and $nCO_2(t)$ correspond to the number of moles of CO_2 in the plug at time t = 0 and t, respectively, and V_S is the volume of the adjacent liquid slug.

Prior to MF experiments, we ensured that physical dissolution of CO_2 in the liquid medium does not change in the presence of FLP reagents. We conducted attenuated total reflection Fourier transform infrared spectroscopy characterization of the physical dissolution of CO_2 in reagent-free bromobenzene, as well as in bromobenzene solutions containing 80 mM tBu$_3$P, 80 mM ClB(C$_6$F$_5$)$_2$, and 160 mM of the FLP reagents (Figure 2a). We monitored the intensity of

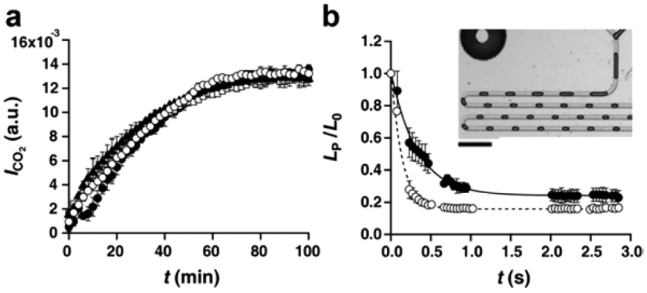

Figure 2. (a) Variation in intensity of the IR band at 2343 cm^{-1} associated with physically dissolved CO_2 in bromobenzene (▲), in a solution of 80 mM tBu$_3$P (□) or 80 mM ClB(C$_6$F$_5$)$_2$ (○) in bromobenzene, and in an equimolar solution of 160 mM tBu$_3$P and ClB(C$_6$F$_5$)$_2$ in bromobenzene (●). (b) Variation in the normalized length of the CO_2 plug with time for the CO_2–bromobenzene (●) and CO_2–FLP solution in bromobenzene at the total FLP concentration of 40 mM FLP (○); T = 293 K. Each experimental point is the average of three results obtained under identical conditions. The inset shows an optical microscopy image of segmented flow with CO_2 plugs (dark color) and slugs of FLP solution in bromobenzene (light color). The scale bar is 500 μm.

the IR peak corresponding to physically dissolved CO_2, I_{CO_2}, at 2343 cm^{-1}. The equilibrium intensity of the peak was reached after 80 min, with identical peak intensity for all the four solutions tested. This result indicated that the physical uptake of CO_2 by bromobenzene was not affected by the presence of individual FLP reagents or a 1:1 mixture of the reagents. On the basis of these results, we used the dissolution of CO_2 in bromobenzene as a reference system for the MF studies of the FLP–CO_2 reaction. We note that the time scale difference between the ATR-FTIR and MF experiments (90 min and 1 s in Figure 2a,b, respectively, needed for liquid saturation with CO_2) is associated with the CO_2 diffusion length difference for these experiments. Similar time scales for both experiments can be achieved if the ATR-FTIR characterization was performed on the same length scale as the MF experiments (Supporting Information, S3).

Figure 2b shows the representative variation in the normalized length, L_P/L_0, of the CO_2 plugs in bromobenzene and an FLP solution, where L_0 is the initial CO_2 plug length formed after the Y-junction. Figure 2, inset, illustrates the shrinkage of CO_2 plugs. Under similar pressure and temperature, the ratio L_P/L_0 was significantly smaller for the system containing FLP reagents than for the FLP-free system, as a result of FLP reaction with CO_2.

Using eqs 1 and 2, we converted the change in volume of the CO_2 plugs into C_{tot} for different FLP concentrations (Figure 3a). With increasing reaction time, t, the concentration of CO_2

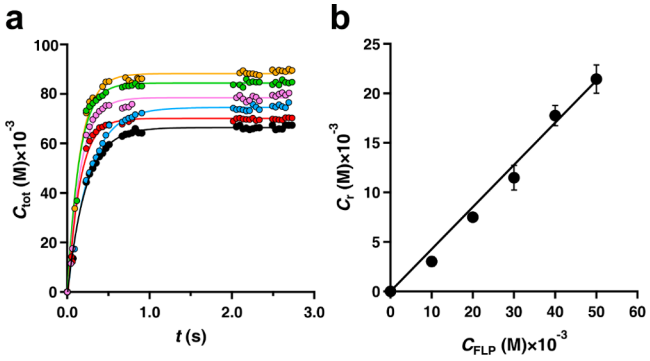

Figure 3. (a) Variation in total molar concentration of CO_2 transferred at 273 K from the gas phase (plugs) to the solution with FLP concentration of 0 mM (black), 10 mM (red), 20 mM (blue), 30 mM (pink), 40 mM (green), and 50 mM (orange). The gaps in the data points appear due to the MF reactor geometry (Supporting Information, Figure S1). (b) Variation in the equilibrium concentration of chemically reacted CO_2, plotted as a function of the initial FLP concentration at T = 273 K. Each experimental point is the average of three experiments conducted under identical conditions. Three hundred images were acquired for each experiment with at least 4000 CO_2 plugs.

in the liquid slugs increased, and the equilibrium was reached after ~2 s. The equilibrium CO_2 uptake by the liquid slugs increased with increasing concentrations of tBu$_3$P and ClB(C$_6$F$_5$)$_2$, indicating that the FLP reagents were the limiting reagents. The CO_2 uptake caused by the chemical reaction, C_r, was determined by subtracting the equilibrium C_{tot} (for the CO_2–bromobenzene system) from the total equilibrium uptake of CO_2, C_{tot}, for the FLP–CO_2 system. Figure 3b shows that the value of C_r increased linearly with FLP concentration.

Since the reaction between ClB(C$_6$F$_5$)$_2$, tBu$_3$P, and CO_2 is exothermic, local heat accumulation immediately downstream of the Y-junction could be expected if the rate of heat generation was faster than heat distribution and dissipation through the walls of the MF reactor. Such accumulation could affect the reaction kinetics and the gas plug size over the course of the reaction but would not affect the thermodynamics of the reaction (see Supporting Information, Figure S4). The

dx.doi.org/10.1021/ja411601a | J. Am. Chem. Soc. 2014, 136, 3875–3880

invariance of CO_2 plug volume after the equilibrium point (Figure 3a) indicated that the heat generated during the CO_2–FLP reaction has been dissipated before the reaction reached the equilibrium.

Following the approach established for the CO_2–FLP reaction at 273 K, we studied the equilibrium chemical uptake of CO_2 by the FLP reagents at 283, 293, 303, and 313 K. The entire MF reactor and a section of the tubings supplying the gaseous CO_2 and the liquid reagents to the MF reactor were immersed in a water bath maintained at the desired temperature. The submersion of the tubing was especially important for the CO_2 gas in order to avoid temperature-mediated, rather than reaction-induced, changes in the CO_2 plug volume. Figure 4 shows that the value of C_r varied linearly with the FLP concentration in the entire temperature range studied.

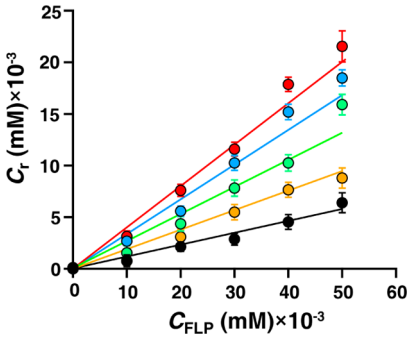

Figure 4. Variation in the equilibrium reaction-induced chemical CO_2 uptake, plotted as a function of the initial concentration of FLP reagents in the adjacent liquid slugs for 273 K (red), 283 K (blue), 293 K (green), 303 K (orange) and 313 K (black).

For similar concentrations of FLP reagents, the value of C_r reduced with increasing temperature. This trend resulted from the reverse FLP–CO_2 reaction, which was favored at elevated temperatures[10] and led to the release of CO_2 from the adduct. As a result, the highest conversion of FLP reagents was achieved at 273 K. Using the data plotted in Figure 4, the equilibrium constant, K_{eq}, of the FLP–CO_2 reaction at a particular temperature was determined as

$$K_{eq} = \frac{[ClB(C_6F_5)_2 - CO_2 - tBu_3P]}{[ClB(C_6F_5)_2][tBu_3P]C_{tot}(\text{bromobenzene})} \quad (3)$$

where $[ClB(C_6F_5)_2–CO_2–tBu_3P]$ is the concentration of the FLP–CO_2 adduct, equal to C_r (determined from Figure 3b), $[ClB(C_6F_5)_2]$ and $[tBu_3P]$ are the equilibrium concentrations of the reagents, calculated as $C_r - [ClB(C_6F_5)_2]_{initial}$ and $C_r - [tBu_3P]_{initial}$, respectively, and C_{tot}(bromobenzene) is the equilibrium concentration of CO_2 dissolved in bromobenzene (Figure 3a). For the calculation of K_{eq}, the reaction of CO_2 with $ClB(C_6F_5)_2$ and tBu_3P was assumed to be stoichiometric and side reactions were ignored. Upon the reaction with FLP reagents, CO_2 is replenished by the continuous dissolution of CO_2 from gaseous plugs, thus maintaining the total supply of CO_2 in the solution. Using eq 3, the equilibrium constants for the FLP–CO_2 reaction carried out at 273, 283, 293, 303, and 313 K were calculated to be 687, 431, 223, 141, and 75 M^{-2}, respectively.

Next, we calculated the Gibbs free energy of the reaction, ΔG, at 273, 283, 293, 303, and 313 K as

$$\Delta G = -RT\ln(K_{eq}) \quad (4)$$

and obtained the values of ΔG to be −14.8, −14.3, −13.2, −12.5, and −11.2 kJ mol^{-1}, respectively.

We then determined the enthalpy and the entropy of the FLP–CO_2 reaction, ΔH and ΔS, by using the van't Hoff equation[36]

$$\ln(K_{eq}) = -\frac{\Delta H^0}{RT} + -\frac{\Delta S^0}{R} \quad (5)$$

and plotting $\ln(K_{eq})$ versus $1/T$, a graph with the slope of $-\Delta H/R$ and the y-intercept of $\Delta S/R$ (Figure 5).

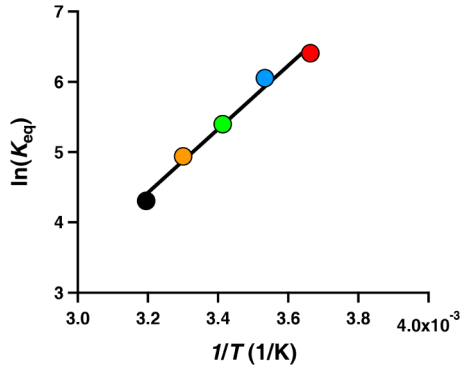

Figure 5. Variation of $\ln(K_{eq})$ with reaction temperature. Based on eq 5, the slope of the graph yields $-\Delta H/R$.

A linear dependence of $\ln(K_{eq})$ versus $1/T$ indicated that ΔH does not appreciably change with temperature over the range studied. The best fit of the linear dependence $\ln(K_{eq})$ versus $1/T$ yielded a ΔH value of −39.3 kJ mol^{-1}. We independently estimated ΔS as $-(\Delta G - \Delta H)/T$ and obtained the values of −89.3, −88.1, −88.8, −88.2, and 89.3 J mol^{-1} K^{-1}, for the temperatures 273, 283, 293, 303, and 313 K, respectively. Table 1 shows the summary of thermodynamic characteristics of the FLP–CO_2 reaction.

Table 1. Thermodynamic Characteristics of the FLP–CO_2 Reaction

T (K)	273	283	293	303	313
K_{eq} (M^{-2})	687	431	223	141	75
ΔH^a (kJ mol^{-1})	−39.3	−39.3	−39.3	−39.3	−39.3
ΔS (J mol^{-1} K^{-1})	−89.3	−88.1	−88.8	−88.2	−89.3
ΔG (kJ mol^{-1})	−14.8	−14.3	−13.2	−12.5	−11.2

[a]The value of ΔH is determined from the slope of the graph in Figure 5.

Finally, we calculated the enhancement factor, E, which describes the influence of a reaction on mass transfer and is defined as the ratio of total absorption of gas by a reactive liquid to the physical absorption of the gas under identical conditions.[37,38] The positive deviation of E from unity reflects the effect of a chemical reaction on increased uptake of a gas by the liquid medium.[39] We determined the value of E as the number of moles of CO_2, $\Delta n_{CO_2,\text{chem-phys}}$, transferred into the FLP solution divided by the number of moles of CO_2, $\Delta n_{CO_2,\text{phys}}$, transferred in bromobenzene as

dx.doi.org/10.1021/ja411601a | J. Am. Chem. Soc. 2014, 136, 3875–3880

$$E = \left(\frac{\Delta n_{CO_2,\text{chem-phys}}}{\Delta n_{CO_2,\text{phys}}} \right) \quad (6)$$

The enhancement factor was determined for different FLP concentrations and different temperatures and is summarized in Table 2. As expected, the value of E increased with an increase in FLP reagent concentration and with decreasing temperature.

Table 2. Enhancement Factor of the FLP−CO_2 Reaction

		[FLP] (mM)				
		10	20	30	40	50
T (K)	273	1.05	1.12	1.18	1.27	1.33
	283	1.04	1.08	1.16	1.23	1.28
	293	1.02	1.06	1.11	1.15	1.23
	303	1.01	1.06	1.10	1.14	1.16
	313	1.01	1.03	1.04	1.07	1.09

We validated the MF methodology by applying it to the well-characterized reaction between CO_2 and diethanolamine and comparing the experimentally obtained enthalpy with the reported literature values. The value of ΔH of −69 kJ mol^{-1} obtained in the MF CO_2−diethanolamine experiments compared favorably with the values of ΔH in the range of −71 ± 4 kJ mol^{-1}, obtained by calorimetry, NMR, and solubility methods (Table S1, Supporting Information).

CONCLUSIONS

In summary, we developed a time- and labor-efficient MF platform for real-time, high-throughput studies of thermodynamics of FLP−CO_2 reactions. The approach presented here was validated for the reaction between CO_2 and diethanolamine. The equilibrium constants, Gibbs energy, enthalpy, and entropy of the FLP−CO_2 reaction were determined at different temperatures. In addition, we determined the enhancement factor under different reaction conditions. The proposed MF strategy provides access to the thermodynamic characterization of FLP−CO_2 reactions that is not accessible otherwise and can be applied to other gas−liquid reactions.

ASSOCIATED CONTENT

Supporting Information

Microfluidic experimental setup, methods of data acquisition and analysis, and infrared spectroscopy experiments. This material is available free of charge via the Internet at http://pubs.acs.org.

AUTHOR INFORMATION

Corresponding Author

ekumache@chem.utoronto.ca

Author Contributions

#D.V. and M.A. contributed equally.

Notes

The authors declare no competing financial interest.

ACKNOWLEDGMENTS

The authors wish to thank Tayseer Mahdi for the synthesis of FLP reagents. A.G., D.W.S., and E.K. are grateful for financial support from NSERC Canada. D.W.S. and E.K. also asknowledge the support of Canada Research Chairs and Carbon Management Canada.

REFERENCES

(1) Sakakura, T.; Choi, J. C.; Yasuda, H. *Chem. Rev.* **2007**, *107*, 2365−2387.
(2) Leitner, W. *Angew. Chem., Int. Ed. Engl.* **1995**, *34*, 2207−2221.
(3) Aresta, M.; Dibenedetto, A. *Dalton Trans.* **2007**, 2975−2992.
(4) Jessop, P. G.; Ikariya, T.; Noyori, R. *Chem. Rev.* **1995**, *95*, 259−272.
(5) Olah, G. A.; Prakash, G.; Goeppert, A. *J. Org. Chem.* **2009**, *74*, 487−498.
(6) Olah, G. A. *Chem. Eng. News* **2003**, *81*, 5.
(7) Nielsen, M.; Alberico, E.; Baumann, W.; Drexler, H. J.; Junge, H.; Gladiali, S.; Beller, M. *Nature* **2013**, *495*, 85−89.
(8) Laitar, D. S.; Muller, P.; Sadighi, J. P. *J. Am. Chem. Soc.* **2005**, *127*, 17196−17197.
(9) Huang, F.; Zhang, C.; Jiang, J.; Wang, Z.; Guan, H. *Inorg. Chem.* **2011**, *50*, 3816−3825.
(10) Bontemps, S.; Vendier, L.; Sabo-Etienne, S. *Angew. Chem., Int. Ed.* **2012**, *51*, 1671−1674.
(11) Sgro, M. S.; Stephan, D. W. *Angew. Chem., Int. Ed.* **2012**, *51*, 11343−11345.
(12) Stephan, D. W.; Erker, G. *Angew. Chem., Int. Ed.* **2010**, *49*, 46−76.
(13) Stephan, D. W. *Dalton Trans.* **2009**, 3129−3136.
(14) Stephan, D. W. *Org. Biomol. Chem.* **2008**, *6*, 1535−1539.
(15) Mömming, C. M.; Otten, E.; Kehr, G.; Fröhlich, R.; Grimme, S.; Stephan, D. W.; Erker, G. *Angew. Chem., Int. Ed.* **2009**, *48*, 6643−6646.
(16) Ashley, A. E.; Thompson, A. L.; O'Hare, D. *Angew. Chem., Int. Ed.* **2009**, *48*, 9839−9843.
(17) Menard, G.; Stephan, D. W. *Dalton Trans* **2013**, *42*, 5447−5453.
(18) Menard, G.; Stephan, D. W. *Angew. Chem., Int. Ed.* **2011**, *50*, 8396−8399.
(19) Menard, G.; Stephan, D. W. *J. Am. Chem. Soc.* **2010**, *132*, 1796−1797.
(20) Dobrovetsky, R.; Stephan, D. W. *Angew. Chem., Int. Ed.* **2013**, *52*, 2516−2519.
(21) Nathanson, G. M.; Davidovits, P.; Worsnop, D. R.; Kolb, C. E. *J. Phys. Chem.* **1996**, *100*, 13007−13020.
(22) Bishnoi, S.; Rochelle, G. T. *Chem. Eng. Sci.* **2000**, *55*, 5531−5543.
(23) Peuser, I.; Neu, R. C.; Zhao, X. X.; Ulrich, M.; Schirmer, B.; Tannert, J. A.; Kehr, G.; Frohlich, R.; Grimme, S.; Erker, G.; Stephan, D. W. *Chem.—Eur. J.* **2011**, *17*, 9640−9650.
(24) Greener, J.; Tumarkin, E.; Debono, M.; Kwan, C.; Abolhasani, M.; Guenther, A.; Kumacheva, E. *Analyst* **2012**, *137*, 444−450.
(25) Kirshnadasan, S.; Brown, R. J. C.; deMello, A. J.; deMello, J. C. *Lab Chip* **2007**, *7*, 1434−1441.
(26) Voicu, D.; Scholl, C.; Li, W.; Jagadeesan, D.; Nasimova, I.; Greener, J.; Kumacheva, E. *Macromolecules* **2012**, *45*, 4469−4475.
(27) Chabinyc, M. L.; Chiu, D. T.; Cooper McDonald, J.; Stroock, A. D. *Anal. Chem.* **2001**, *73*, 4491−4498.
(28) Song, H.; Ismagilov, R. F. *J. Am. Chem. Soc.* **2003**, *125*, 14613−14619.
(29) Ristenpart, W. D.; Wan, J.; Stone, H. A. *Anal. Chem.* **2008**, *80*, 3270−3276.
(30) Nguyen, D. T.; Leho, Y. T.; Esser-Kahn, A. P. *Adv. Funct. Mater.* **2013**, *23*, 100−106.
(31) Li, W.; Liu, K.; Simms, R.; Greener, J.; Jagadeesan, D.; Pinto, S.; Guenther, A.; Kumacheva, E. *J. Am. Chem. Soc.* **2011**, *134*, 3127−3132.
(32) Lefortier, S. G. R.; Hamersma, P. J.; Bardow, A.; Kreutzer, M. T. *Lab Chip* **2012**, *12*, 3387−3391.
(33) Sun, R.; Cubaud, T. *Lab Chip* **2011**, *11*, 2924−2928.
(34) Abolhasani, M.; Singh, M.; Kumacheva, E.; Guenther, A. *Lab Chip* **2012**, *12*, 1611−1618.
(35) Abolhasani, M.; Singh, M.; Kumacheva, E.; Guenther, A. *Lab Chip* **2012**, *12*, 4787−4795.
(36) Atkins, P.; de Paula, J. *Physical Chemistry*; W.H. Freeman: New York, 2006; pp 212−215.
(37) Doraiswamy, L. K.; Sharma, M. M. *Heterogeneous Reactions: Fluid−Fluid−Solid Reactions*; Wiley: New York, 1984.

(38) Hogendoorn, J. A.; Vas Bhat, R. D.; Kuipers, J. A. M.; van Swaaij, W. P. M.; Versteeg, G. F. *Chem. Eng. Sci.* **1997**, *52*, 4547−4559.
(39) Shao, N.; Gavriilidis, A.; Angeli, P. *Chem. Eng. J.* **2010**, *160*, 873−881.